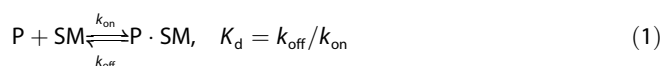


DOI: 10.1002/cbic.201100617

Kinetic Capillary Electrophoresis with Mass-Spectrometry Detection (KCE-MS) Facilitates Label-Free Solution-Based Kinetic Analysis of Protein–Small Molecule Binding

Jiayin Bao, Svetlana M. Krylova, Derek J. Wilson, Oren Reinstein, Philip E. Johnson, and Sergey N. Krylov[✉][a]

Small molecules regulate many important cellular processes through binding to proteins,^[1] thus, many modern small-molecule drugs are developed to bind selectively to protein targets and change their function.^[2] Understanding the dynamics of both cellular regulation by small molecules and small-molecule-drug action requires knowing the kinetic rate constants, k_{on} and k_{off} , of interaction between a protein (P) and a small molecule (SM) with the formation of their noncovalent complex (P·SM).^[3]



K_d is the equilibrium dissociation constant for this reaction.

There are label-free, solution-based equilibrium methods that can measure the K_d of protein–small molecule interactions.^[4] Examples include classical isothermal titration calorimetry (ITC),^[5] saturation transfer difference spectroscopy,^[6] and affinity capillary electrophoresis,^[7] as well as, more recent, electrospray mass spectrometry-based diffusion,^[8] protein ligand interaction by mass spectrometry, titration, and H/D exchange (PLIM-STEEX),^[9] and thermophoresis.^[10] The kinetic methods used for measuring k_{on} and k_{off} of protein–small molecule interactions are either surface-based (e.g., surface plasmon resonance (SPR)^[11] and biolayer interferometry^[12]) or label-based (e.g., stopped-flow spectroscopy^[13]). Surface-based methods require the immobilization of either the protein or the small molecule on the surface of a sensor. The label-based methods require the modification of either the protein or the small molecule with a spectroscopically detectable label, typically a fluorophore. It is evident that both modifications can drastically affect k_{on} and k_{off} and are very cumbersome if the small molecule is to be immobilized or labeled. Unfortunately, according to fundamental physics, the most sensitive mode of detection usually requires the immobilization or labeling of the small molecule rather than the protein.^[14]

While surface- and label-based methods with immobilized and labeled proteins can be used to measure k_{on} and k_{off} for protein–small molecule interactions,^[11–13] such measurements would be simpler and more accurate if solution-based, label-free methods were available. Here we report on the first such method, which combines kinetic capillary electrophoresis (KCE) separation^[15] with mass spectrometry detection. KCE and MS were interfaced in a way that kept the quantitative capabilities of both methods and allowed us to determine k_{on} and k_{off} for the interaction of four protein–small molecule pairs. KCE-MS was validated by comparing the K_d measured by KCE-MS with that measured by ITC. The results suggest that KCE-MS is a promising platform for the development of practical label-free, solution-based methods for studying the kinetics of affinity interactions.

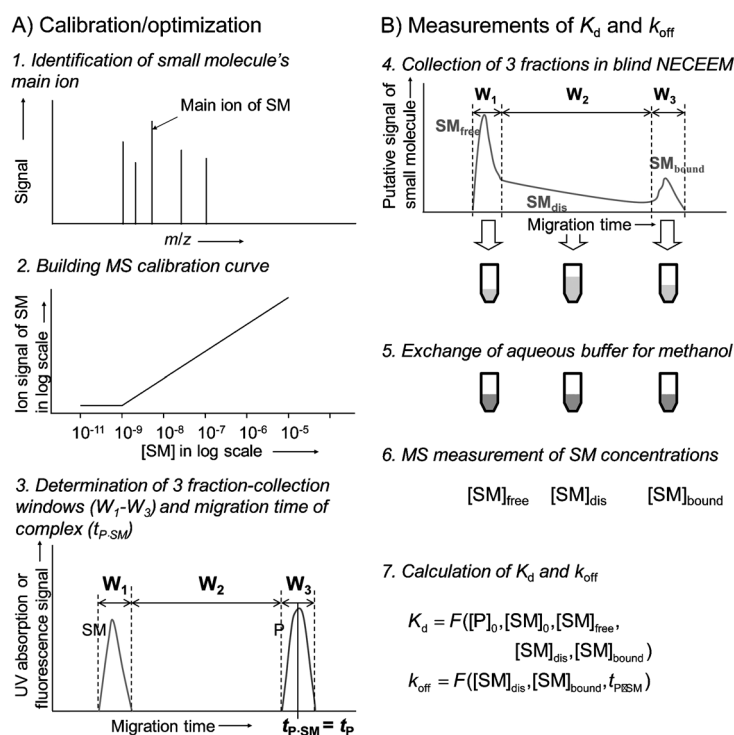


Figure 1. Schematic description of the practical realization of KCE-MS through off-line interfacing of NECEEM with ESI-TOF MS. See text for details.

[a] J. Bao, Dr. S. M. Krylova, Prof. D. J. Wilson, O. Reinstein, Prof. Dr. P. E. Johnson, Prof. Dr. S. N. Krylov
Department of Chemistry and
Centre for Research on Biomolecular Interactions
York University 4700 Keele Street, Toronto, Ontario M3J 1P3 (Canada)
E-mail: skrylov@yorku.ca

Supporting information for this article is available on the WWW under <http://dx.doi.org/10.1002/cbic.201100617>.

Figure 1 explains our practical realization of the general KCE-MS approach with a KCE method known as nonequilibrium capillary electrophoresis of equilibrium mixtures (NECEEM),^[16] and quadrupole-TOF MS with electrospray ionization (ESI).^[17]

In the NECEEM method, the small molecule is mixed with the protein, and they are incubated so as to approach equilib-

rium. Such an equilibrium mixture contains three components: unbound small molecule, unbound protein, and the protein–small molecule complex. The amounts of the three components are controlled by the equilibrium dissociation constant, K_d . An aliquot of the equilibrium mixture is pressure injected into a capillary, and a high voltage is applied to separate the three components from each other. The separation disturbs the equilibrium, and the complex dissociates during the course of electrophoresis with a monomolecular rate constant k_{off} . If only the small molecule is detected at the capillary exit, the NECEEM electropherogram comprises three characteristic areas corresponding to: 1) the small molecule that was unbound in the equilibrium mixture, 2) the small molecule that dissociated from the complex during the course of electrophoresis, and 3) the small molecule still bound to the protein at the time it reaches the capillary exit. The three areas can be used to calculate k_{off} and K_d through simple algebraic formulas (see below).

There are three major calibration/optimization steps (Figure 1A). In step 1, the dominant ion for the small molecule to be studied is determined by spraying pure small molecule into the mass spectrometer. In step 2, the ion intensity is related to concentration by using a serial-dilution calibration curve. Step 3 is to determine the three fraction-collection windows (W_1 , W_2 , and W_3) and the migration time of the complex, $t_{p,SM}$ (used in k_{off} calculation) required for the next steps by using CE with UV light absorption detection. To increase the accuracy of the results in step 3, the small molecule and the protein are sampled for CE analysis separately at high concentration. The migration time of the complex is assumed to be the same as that of the protein for two reasons. First, the differences in the molecular sizes and charges of the complex and the protein are not significant (typically less than 10%). Second, the velocity of the electroosmotic flow (EOF) is much greater than the electrophoretic velocity of the protein. Thus, even if the binding slightly changes the electrophoretic mobility of the protein, the migration time will not change appreciably. Therefore, $t_{p,SM}$ can be determined as the migration time of the pure protein, t_p . We recently tested the influence of protein labeling with multiple fluorophore molecules on a single protein and found that, even after such a significant change in size, the change in protein mobility was insignificant.^[18] In addition, the negligible influence of small molecule binding to the protein on protein mobility can be confirmed experimentally by optically detecting the protein peak in the presence and absence of the small molecule.

The three calibration/optimization steps are followed by four steps involved in actually measuring the binding parameters (Figure 1B). The equilibrium mixture of protein and small molecule is prepared with a CE internal standard, fluorescein (this might be needed to correct the positions of the fraction-collection windows if the protein changes the velocity of EOF). In step 4, an aliquot of the equilibrium mixture is sampled for NECEEM, and three fractions are blindly collected—by using the fraction-collection windows determined in step 3—into tubes containing identical amounts of an MS internal standard, metoprolol (the MS internal standard is needed to calibrate for fluctuations in ESI efficiency within and between MS runs). As

schematically illustrated in Figure 1B, fraction 1 contains the small molecule that was unbound in the equilibrium mixture; fraction 2 contains the small molecule that dissociated from the complex during electrophoretic separation, and fraction 3 contains the small molecule that is still within intact protein–small molecule complexes. NECEEM is performed in a buffer at close to physiological pH, which is not suitable for ESI-MS. In order to use collected fractions in the subsequent MS analysis, the fractions are desalted, and the small molecule is dissolved in equal volumes of methanol (step 5). In step 6, the concentrations of the small molecule in the three fractions, $[SM]_{free}$, $[SM]_{dis}$, $[SM]_{bound}$ are measured by MS. The MS internal standard facilitates accurate small molecule quantitation. Since the volumes of the three sampled solutions are identical, the concentrations are proportional to the total amounts of the small molecule in the fractions. Accordingly, in step 7, the three concentrations are used instead of amounts to calculate K_d and k_{off} with simple NECEEM formulas:^[16]

$$K_d = \frac{[P]_0 - [SM]_0 \left(1 - \frac{[SM]_{free}}{[SM]_{free} + [SM]_{dis} + [SM]_{bound}} \right)}{\frac{[SM]_{free} + [SM]_{dis} + [SM]_{bound}}{[SM]_{free}} - 1} \quad (2)$$

$$k_{off} = \ln \left(\frac{[SM]_{dis} + [SM]_{bound}}{[SM]_{bound}} \right) / t_{p,SM} \quad (3)$$

The formulas also utilize the concentrations of the small molecule, $[SM]_0$, and protein, $[P]_0$, used to prepare the initial equilibrium mixture and the migration time of the complex, $t_{p,SM}$, determined in step 3. The entire procedure of KCE-MS is straightforward and six repeats can be performed in 17 h.

To validate the KCE-MS procedure depicted in Figure 1, we used the interaction between alpha 1 acid glycoprotein (AGP) and four small molecules: propranolol, alprenolol, labetalol, and pindolol. AGP is a highly abundant plasma protein with a typical concentration of 0.4–1.0 g L⁻¹; it is the major binding protein for cationic small molecules in the human body.^[19,20] Figure 2 shows calibration/optimization of MS for propranolol.

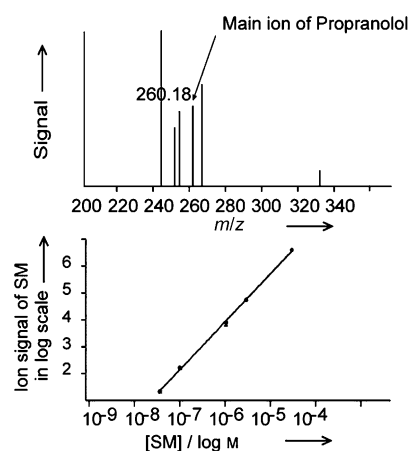


Figure 2. Determination of propranolol by mass spectrometry: mass spectrum (top) and calibration curve (bottom). See the Supporting Information for technical details.

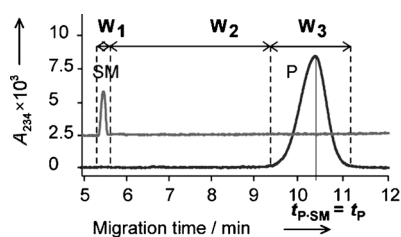


Figure 3. Determination of fraction-collection windows and migration time of the protein, $t_p = t_{p,SM}$, for the AGP–propranolol interacting pair by CE. The propranolol electropherogram (upper line) has been offset vertically by $+0.0025$ absorbance units for clarity of viewing. See the Supporting Information for technical details.

Figure 3 illustrates the determination of the three fraction-collection windows for studying the interaction between AGP and propranolol. It also shows the migration time of the protein, $t_p = t_{p,SM}$, which is used in the formula for k_{off} . Similar results for the other three small molecules are shown in Figure S1 in the Supporting Information. After completing the calibration/optimization steps, we conducted KCE-MS using the sequence depicted in Figure 1B with six repeats for every interacting pair. We also conducted ITC-based measurements of K_d values for the four interacting pairs in triplicate (an example thermogram for propranolol is shown in Figure S2).

Table 1 summarizes the results for all KCE-MS and ITC measurements. The K_d values derived from the two methods were similar for propranolol and for alprenolol, but differed by fac-

Table 1. Binding parameters for the interaction of AGP with four small molecules measured by KCE-MS and ITC.				
Small molecule	k_{off} [s^{-1}]	KCE-MS K_d [μM]	$k_{on}^{[a]}$ [$M^{-1} s^{-1}$]	ITC K_d [μM]
propranolol	$(1.9 \pm 0.9) \times 10^{-3}$	5.5 ± 3.7	$(5.1 \pm 3.8) \times 10^2$	7.0 ± 1.9
alprenolol	$(1.9 \pm 0.1) \times 10^{-3}$	2.1 ± 0.3	$(9.2 \pm 1.1) \times 10^2$	4.6 ± 3.2
labetalol	$(2.4 \pm 0.3) \times 10^{-3}$	82.7 ± 10.7	$(2.9 \pm 0.4) \times 10^1$	17.4 ± 1.7
pindolol	$(3.4 \pm 0.2) \times 10^{-3}$	17.6 ± 1.5	$(2.0 \pm 0.3) \times 10^2$	7.7 ± 3.1

[a] Calculated as k_{off}/K_d .

tors of 5 and 2 for labetalol and pindolol, respectively. It is known that conceptually different evaluation methods can give considerably different equilibrium constants.^[21] Moreover, the deviation is dependent on the molecules studied.^[22] ITC and KCE-MS are conceptually different methods that utilize different physical principles and are characterized by unique sources of errors. This is likely the explanation for differences between the KCE-MS- and ITC-measured K_d values for labetalol and pindolol. At this time, this is the best explanation we can offer. Although it is worth mentioning that previously published results obtained with another label-free method (affinity CE) are closer to the KCE-MS results: $46 \mu M$ for labetalol and $33 \mu M$ for pindolol.^[20] We thus conclude that this initial validation of KCE-MS is satisfactory and sufficient to continue efforts in further development of this new method.

In contrast to all other label-free, solution-based methods, the KCE-MS method can also facilitate the determination of the kinetic rate constant, k_{off} . Since the calculation of k_{off} by KCE-MS uses the same data for the concentrations of the small molecule as the calculation of K_d , we suggest that the partial agreement of K_d measured by KCE-MS and ITC indirectly confirms the validity of k_{off} data. The only additional parameter used in k_{off} determination is the migration time of the complex, which can be found very accurately by running a control CE experiment with protein only. Hence, ITC validation also suggests that k_{off} is measured accurately by KCE-MS. To the best of our knowledge, the values of k_{off} and k_{on} were determined for the above interacting pairs in a label-free, solution-based fashion for the first time.

To conclude, we have outlined the main features of KCE-MS. KCE-MS is introduced as a platform for the development of label-free solution-based methods for studying the kinetics of protein–small molecule interactions. The method follows the migration pattern of a small molecule in KCE by means of MS detection. In this proof-of-principle work, we interfaced KCE and MS off-line, which allowed us to integrate a simple desalting/buffer-exchange procedure between KCE and MS. Our proof of principle suggests that efforts towards on-line interfacing of KCE and MS are justified. The method requires that the protein and small molecule be separated in capillary electrophoresis. This could be a method limitation when the electrophoretic mobilities of the protein and small molecule are coincidentally very similar. Measuring fast reactions with low K_d values will require low concentrations of interacting molecules and, accordingly, a lower MS detection limit. The range of k_{on} , k_{off} , and K_d that can be measured by KCE-MS will depend on the efficiency of the protein and small-molecule separation in KCE and on the MS detection limit. Instrumentation for KCE-MS used in this study can measure K_d values as low as approximately 30 nM (see calibration curves). Measuring sub-nanomolar K_d values will require a mass spectrometer with a sub-nanomolar detection limit. The best contemporary MS instruments have limits of detection in the zeptomolar range.

The accuracy of kinetic measurements in KCE-MS depends on the correctness of the determination of the fraction-collection windows. The kinetic results are less sensitive to shifting of the outer boundaries and more sensitive to shifting of the inner boundaries (see Figure S3 in the Supporting Information for more details). Advantageously, KCE-MS does not require MS detection of an intact protein–small molecule complex, which can be very challenging. The ability of MS to rapidly scan through m/z can facilitate the simultaneous analysis of one protein with several small molecules and multiple interacting pairs; this would potentially lead to high-throughput screening of panels of drug candidates. We also foresee that the method will be used in kinetic studies of interacting molecules other than a protein and a small molecule.

Experimental Section

Chemicals and materials: Fused-silica capillaries were purchased from Polymicro (Phoenix, AZ, USA). Human α_1 -acid glycoprotein

(AGP), labetalol hydrochloride, (\pm)-metoprolol (+)-tartrate salt, alprenolol hydrochloride, pindolol, (+)-propranolol hydrochloride, and Tris base were purchased from Sigma–Aldrich. All reagents were dissolved in Tris A buffer (25 mM Tris-acetate, pH 7.2). The collection buffer was Tris A with metoprolol (100 nM). All solutions were made with deionized water filtered through a 0.22 μ m filter (Millipore).

Instrumentation: All capillary electrophoresis CE experiments were carried out on an MDQ-PACE instrument (Beckman–Coulter, ON, Canada) equipped with photodiode array (PDA) detector. PDA data were recorded at 234, 226, and 260 nm with a 4 Hz acquisition rate. The inner and outer diameters of the capillary were 100 and 360 μ m, respectively. For CE UV detection experiment, a 60.5 cm capillary was used with 50.3 cm length from the injection end to the detection window. MS experiments were carried out on a QStar Elite quadrupole time-of-flight (Q-TOF) instrument (AB Sciex, Concord, ON, Canada) with a commercial ionization source. Samples were injected and delivered by using Harvard 11+ infusion syringe pumps (Holliston, MA, USA) at a rate of 5 μ L min⁻¹. Isothermal titration calorimetry (ITC) experiments were performed on a MicroCal VP-ITC instrument (Northampton, MA, USA). The MicroCal Thermo Vac unit (Northampton, MA, USA) was used for sample degassing.

CE experiments: The Tris A buffer was used for both incubation and separation. The concentrations of the small molecules were 20 μ M propranolol, 20 μ M alprenolol, 30 μ M pindolol, and 40 μ M labetalol. In NECEEM experiments, each “equilibrium mixture” contained equal concentrations of the protein and the small molecule. The capillary was flushed prior to each CE run with HCl (0.1 M), NaOH (0.1 M), ddH₂O, and Tris A buffer. The sample (123 nL) was injected into the capillary by applying a pressure pulse of 3450 Pa for 10 s. A pressure of 690 Pa was then applied for 2.5 min to move the sample through the inefficiently cooled region of the capillary. Finally, electrophoresis was driven by an electric field of 500 V cm⁻¹. Electropherograms were analyzed with 32 Karat software. In NECEEM experiments, fractions were collected into the collection buffer (20 μ L), lyophilized for 2 h, and stored at -80 °C.

Electrospray ionization mass spectrometry (ESI-MS) analysis: Samples were dissolved in HPLC-grade methanol (100 μ L) before being delivered into the spectrometer. The source was rinsed with ddH₂O and HPLC-grade methanol prior to each injection. The ion source potential was +5100 V, and optimal acceleration and focusing conditions were achieved by using 60 V declustering potential and 275 V focusing potential. The samples were scanned over 200–350 *m/z* for 5 min at one spectrum per second in a multichannel accumulation (MCA) mode. The results were analyzed by using Analyst QS 2.0 software.

Isothermal titration calorimetry analysis: All samples were prepared in Tris A buffer. Binding experiments were conducted at 20 °C on protein (20–88 μ M) and small molecules (0.64–9.4 mM). The experimental setup consisted of either 1) 35 successive injections (8 μ L) of small molecule into protein every 300 s to a final molar ratio of 3:1 or 2) 19 successive injections (3 μ L) of small molecule into protein followed by 15 injections of small molecule (15 μ L) to a final molar ratio of 30:1. The first injection was 2 μ L for all experiments. All experiments were corrected for the heat of dilution of the titrant. Data were acquired from *c* values ranging between 2.5 and 27. Data analysis was carried out with Origin 5.0 software by using a single-site binding model.

Acknowledgements

This work was supported by the NSERC Canada.

Keywords: electrophoresis • label-free kinetics assays • mass spectrometry • proteins • small molecules

- [1] A. J. Firestone, J. K. Chen, *ACS Chem. Biol.* **2010**, *5*, 15–34.
- [2] a) B. Lomenick, R. W. Olsen, J. Huang, *ACS Chem. Biol.* **2011**, *6*, 34–46; b) A. C. Backes, B. Zech, B. Felber, B. Klebl, G. Müller, *Expert Opin. Drug Discovery* **2008**, *3*, 1409–1425; c) V. V. Vintonyak, H. Waldmann, D. Rauh, *Bioorg. Med. Chem.* **2011**, *19*, 2145–2155; d) P. Imming, C. Sinning, A. Meyer, *Nat. Rev. Drug Discovery* **2006**, *5*, 821–834.
- [3] D. C. Swinney, *Drug Discovery* **2010**, *7*, 53–57.
- [4] M. A. Cooper, *Anal. Bioanal. Chem.* **2003**, *377*, 834–842.
- [5] a) R. J. Falconer, B. M. Collins, *J. Mol. Recognit.* **2011**, *24*, 1–16; b) Y. Liang, *Acta Biochim. Biophys. Sin.* **2008**, *40*, 565–576.
- [6] B. Meyer, T. Peters, *Angew. Chem.* **2003**, *115*, 890–918; *Angew. Chem. Int. Ed.* **2003**, *42*, 864–890.
- [7] S. Kiessig, F. Thuncke in *Affinity Capillary Electrophoresis in Pharmaceuticals and Biopharmaceutics* (Eds.: R. H. H. Neubert, H. H. Ruttinger), Marcel Dekker, New York, **2003**, pp. 211–241.
- [8] S. M. Clark, L. Konermann, *Anal. Chem.* **2004**, *76*, 7077–7083.
- [9] a) M. M. Zhu, D. L. Rempel, Z. H. Du, M. L. Gross, *J. Am. Chem. Soc.* **2003**, *125*, 5252–5253; b) T. Tu, M. Dragusanu, B.-A. Petre, D. L. Rempel, M. Przybylski, M. L. Gross, *J. Am. Soc. Mass Spectrom.* **2010**, *21*, 1660–1667.
- [10] a) P. Baaske, C. J. Wienken, P. Reineck, S. Dühr, D. Braun, *Angew. Chem.* **2010**, *122*, 2286–2290; *Angew. Chem. Int. Ed.* **2010**, *49*, 2238–2241; b) C. J. Wienken, P. Baaske, U. Rothbauer, D. Braun, S. Dühr, *Nat. Commun.* **2010**, *1*, 100.
- [11] a) R. L. Rich, L. R. Hoth, K. F. Geoghegan, T. A. Brown, P. K. LeMotte, S. P. Simons, P. Hensley, D. G. Myszka, *Proc. Natl. Acad. Sci. USA* **2002**, *99*, 8562–8567; b) Y. S. N. Day, C. L. Baird, R. L. Rich, D. G. Myszka, *Protein Sci.* **2002**, *11*, 1017–1025; c) D. G. Myszka, *Anal. Biochem.* **2004**, *329*, 316–323.
- [12] C. A. Wartchow, F. Podlaski, S. Li, K. Rowan, X. Zhang, D. Mark, K.-S. Huang, *J. Comput. Aided Mol. Des.* **2011**, *25*, 669–676.
- [13] a) J. Lew, S. S. Taylor, J. A. Adams, *Biochemistry* **1997**, *36*, 6717–6724; b) R. Murugan, S. Mazumdar, *Arch. Biochem. Biophys.* **2006**, *455*, 154–162.
- [14] a) N. Kanoh, M. Kyo, K. Inamori, A. Ando, A. Asami, A. Nakao, H. Osada, *Anal. Chem.* **2006**, *78*, 2226–2230; b) R. P. H. Kooyman in *Handbook of Surface Plasmon Resonance* (Eds.: R. B. M. Schasfoort, A. J. Tudos), RSC Publishing, Cambridge, **2008**, pp. 15–35.
- [15] a) A. Petrov, V. Okhonin, M. Berezovski, S. N. Krylov, *J. Am. Chem. Soc.* **2005**, *127*, 17104–17110; b) S. N. Krylov, *Electrophoresis* **2007**, *28*, 69–88.
- [16] a) M. Berezovski, S. N. Krylov, *J. Am. Chem. Soc.* **2002**, *124*, 13674–13675; b) S. N. Krylov, *J. Biomol. Screening* **2006**, *11*, 115–122.
- [17] I. V. Chernushevich, A. V. Loboda, B. A. Thomson, *J. Mass Spectrom.* **2001**, *36*, 849–865.
- [18] S. de Jong, S. N. Krylov, *Anal. Chem.* **2011**, *83*, 6330–6335.
- [19] S. S. Gustafsson, L. Vrang, Y. Terelius, U. H. Danielson, *Anal. Biochem.* **2011**, *409*, 163–175.
- [20] M. A. Martínez-Gómez, S. Sagrado, R. M. Villanueva-Camañas, M. J. Medina-Hernández, *Electrophoresis* **2006**, *27*, 3410–3419.
- [21] M. C. Jecklin, S. Schauer, C. E. Dumelin, R. Zenobi, *J. Mol. Recognit.* **2009**, *22*, 319–329.
- [22] H. Fuchs, R. Gessner, *Biochem. J.* **2001**, *359*, 411–418.

Received: September 29, 2011

Published online on October 19, 2011

Supporting Figures

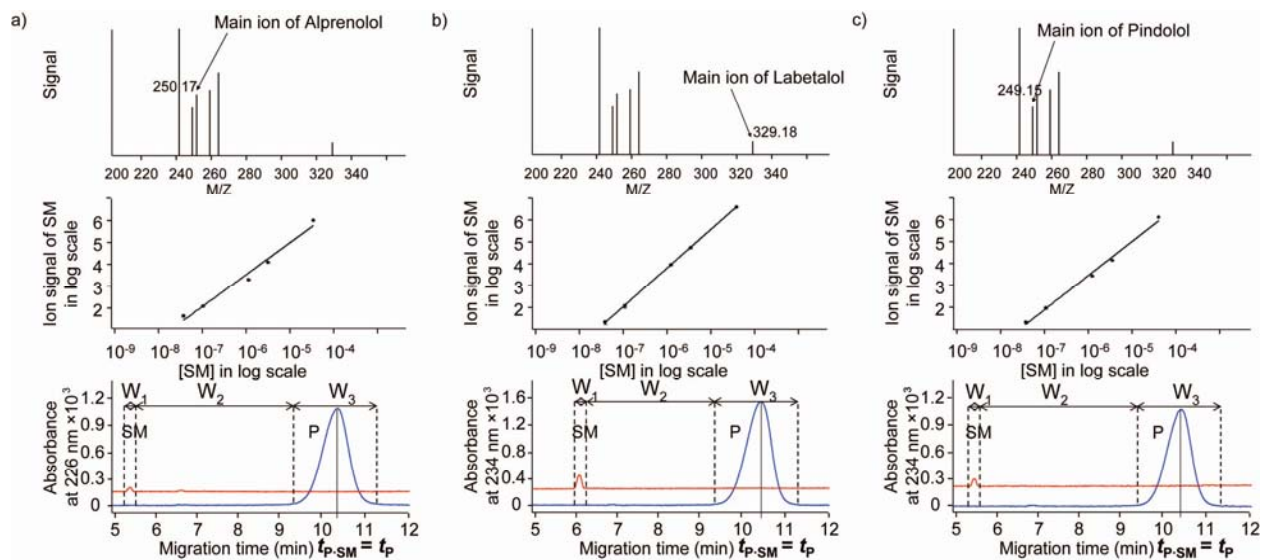


Figure S1. Mass spectrometry determination and fraction collection of small molecules. Panels **a**, **b**, and **c** represents the data for alprenolol, labetalol and pindolol, respectively. Top panels illustrate small molecules determination by MS. Middle panels are MS calibration curves for each small molecule. Bottom panels illustrate the determination of the 3 fractions-collection windows and the migration time of AGP-small molecule complex, $t_P = t_{P-SM}$. Traces of small molecules (red) are offset vertically by 0.0025 absorbance units for clarity of viewing.

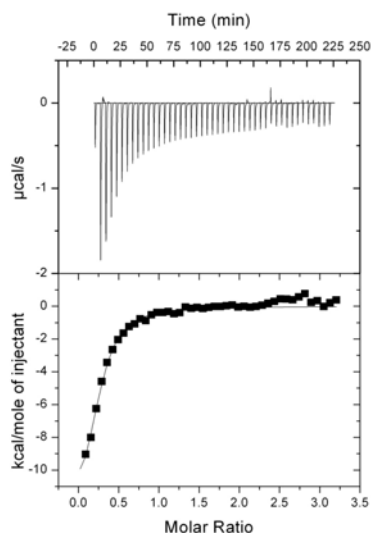


Figure S2. Thermogram of propranolol binding by AGP monitored by ITC. The top box shows the raw ITC data acquired in real time. In the bottom box, the data is integrated with respect to time displaying total heat per injection. The fit was generated using the one-site binding model.

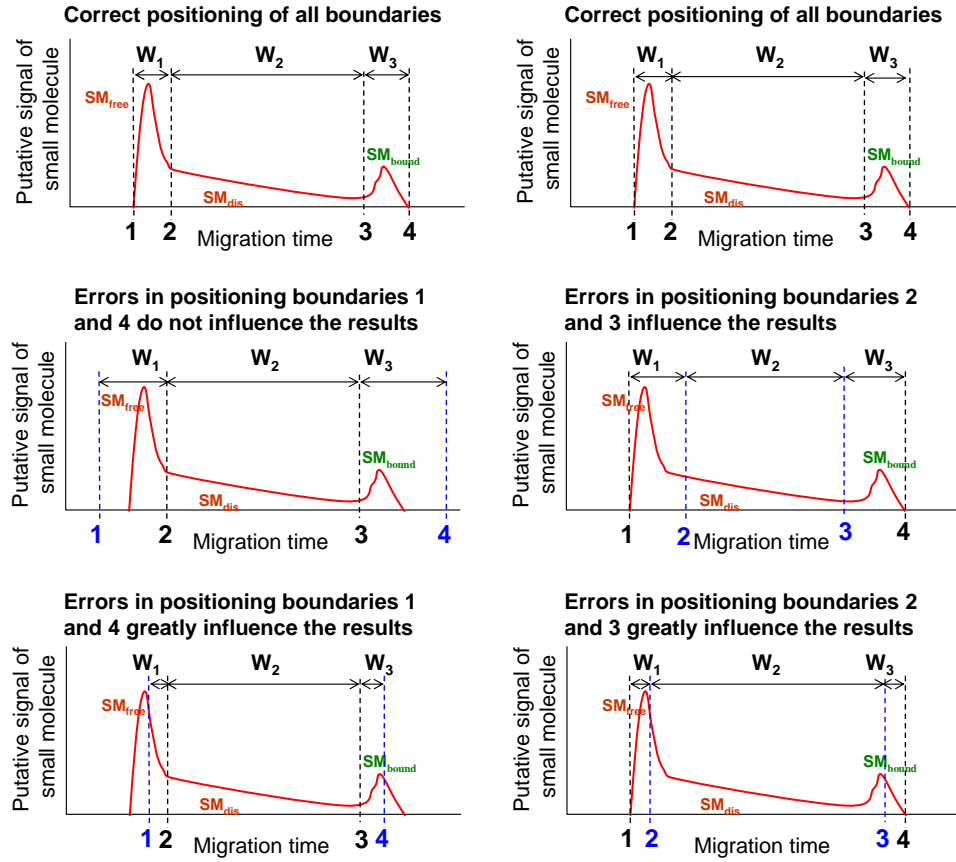


Figure S3. Schematic illustration of the influence of boundary positioning on the accuracy of kinetic analysis of protein-small molecule binding by KCE-MS. The top panels show the correct positioning of boundaries 1-4. The middle and bottom panels show the incorrect positioning of the boundaries and qualitative assessment of the influence of the error in positioning on the kinetic measurements.